Improved noninterferometric test of collapse models using ultracold cantilevers: Supplemental Material

A. Vinante,[1] R. Mezzena,[2] P. Falferi,[1] M. Carlesso,[3,4] and A. Bassi[3,4]

[1]*Istituto di Fotonica e Nanotecnologie, CNR - Fondazione Bruno Kessler, I-38123 Povo, Trento, Italy.*
[2]*Department of Physics, University of Trento, I-38123 Povo, Trento, Italy.*
[3]*Department of Physics, University of Trieste, Strada Costiera 11, 34151 Trieste, Italy*
[4]*Istituto Nazionale di Fisica Nucleare, Trieste Section, Via Valerio 2, 34127 Trieste, Italy*

CSL FORCE NOISE

The expression for the CSL-induced force noise spectral density can be obtained directly from the correlations of the CSL force on the system [17,21]. In terms of the CSL parameters and the mass density distribution $\mu(\boldsymbol{r})$ of the system, the one-sided spectral density S_F reads:

$$S_F = \frac{2\hbar^2\lambda r_C^3}{\pi^{3/2}m_0^2}\int \mathrm{d}\boldsymbol{k}\, k_x^2 e^{-k^2r_C^2}|\tilde{\mu}(\boldsymbol{k})|^2, \qquad \text{(S1)}$$

where $\tilde{\mu}(\boldsymbol{k})$ is the Fourier transform of $\mu(\boldsymbol{r})$ and x is the direction of the monitored oscillations of the system.

In Ref. [17], a normalized diffusion constant η was derived, which coincides with the force noise apart from a constant factor, according to the relation $S_F = 2\hbar^2\eta$. Here, the factor 2 originates from the fact that in the experiment we use the one-sided definition of spectral density. For the cantilever-microsphere system the integration can be carried out exactly as done in Ref. [17], as the geometry is the same. For a given measured residual force noise S_{F0} the exclusion plot in the CSL parameter space is obtained by comparing S_{F0} with Eq. (S1).

ADDITIONAL INFORMATION ON FITTING THE NOISE SPECTRA

The power spectra of the SQUID output signal are experimentally obtained by averaging a number, typically $n_{\mathrm{av}} = 120$, of power FFT periodograms of the SQUID signal. The sampling frequency was set to $f_s = 100$ kHz and the length of each dataset was 2^{20} samples, corresponding to a frame period of $t_f = 10.49$ s and a frequency resolution $df = 95.36$ mHz.

Each averaged spectrum is fitted with a weighted nonlinear Levenberg-Marquardt procedure on the fixed interval $8100 - 8240$ Hz, using Eq. (2) as template and setting the relative error bar of each bin as $1/\sqrt{n_{\mathrm{av}}}$. As it is usually difficult to fit very narrow resonance peaks, we fix the parameters f_0, f_1 and Q to the values independently determined by ringdown and calibration measurements, leaving only A,B and C as free parameters. A and C are mainly determined by the SQUID noise, while B is mainly determined by the tails of the resonant peak.

The fits are typically good, according to a standard χ^2 test. In Fig. S1 we plot the residuals of the fits, normalized by the error bar, for the three representative spectra shown in Fig. 2. In general, no systematic discrepancy between the fitted function and the data is observed, except for a small reproducible imperfect fitting exactly around the resonance frequency of 8174.0 Hz. This feature can be explained as a data processing artifact due to spectral leakage. In fact, the width of the resonance peak $\Delta f = f_0/Q_a \simeq 50$ mHz is comparable to the spectrum resolution, so that there is a slight broadening, typically non Lorentzian, of the $3-5$ points at the very top of the peak. This localized imperfection leads to a slight increase of the value of χ^2, however it does not significantly affect the fit results. In fact, with the parametrization of Eq. (2), the B parameter is determined by the whole tails of the resonant peak, while the top part is determined by the fixed Q_a factor. In other words, by fitting with Eq. (2) we use the information on the cantilever noise available over the whole noise bandwidth (roughly 20 Hz). This would not be the case for a measurement strategy aiming at measuring the total integrated cantilever noise.

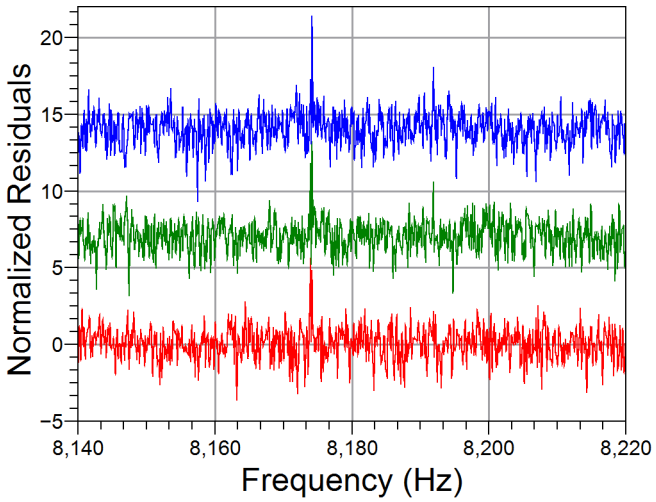

FIG. S1: Normalized fit residuals for the three representative spectra shown in Fig. 2. From bottom to top, $T = 43, 171, 351$ mK respectively. The residuals at 171 and 351 mK are shifted from 0 for a better visualization.

In Fig. S2 we plot the reduced χ^2 (with 1460 degrees of freedom) of all fits, obtained after exclusion of the 5 points around the resonance. The gray region repre-

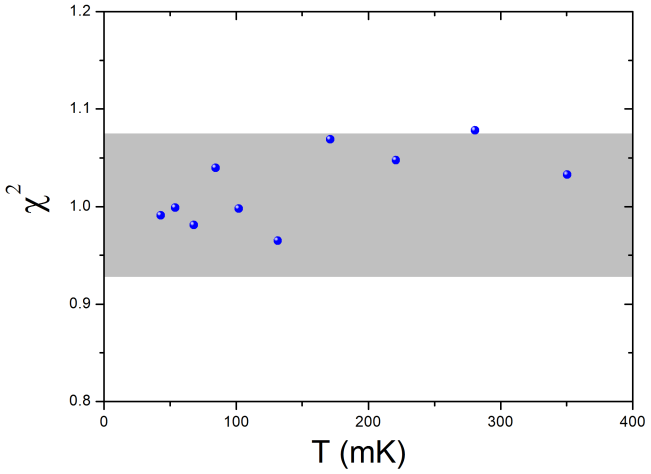

FIG. S2: Reduced χ^2 of the fits, compared with the theoretical two-sided 2σ interval (light gray region) of the reduced χ^2 distribution with the same number of degrees of freedom.

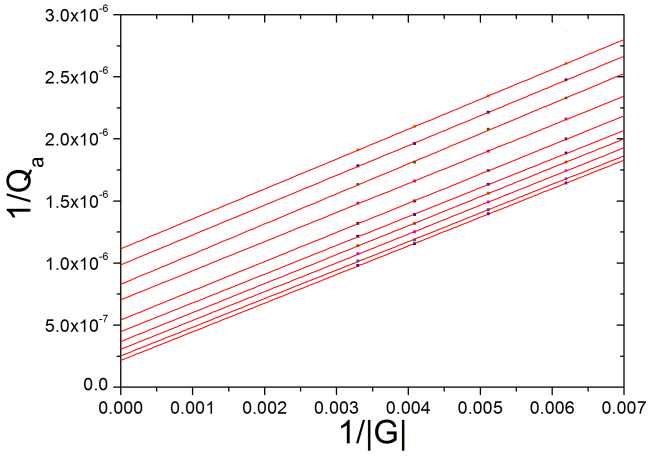

FIG. S3: Inverse of the apparent quality factor Q_a, estimated by ringdown measurements, as function of the inverse of the open loop gain $|G|$ of the SQUID feedback electronics. Each dataset refers to a different temperature: from top to bottom 43,54,68,84,102,132,171,221,281,351 mK. These temperatures correspond to the noise measurements shown in Fig. 3. The intercept of each linear fit provides an estimate of the intrinsic quality factor at the corresponding temperature.

sents the theoretical two-sided 2σ interval of the reduced χ^2 distribution. The experimental χ^2 is essentially in agreement with the theoretical distribution, with only one point slightly beyond the 2σ limit.

ESTIMATION OF THE INTRINSIC QUALITY FACTOR

The knowledge of the intrinsic quality factor Q is essential in order to evaluate the factor T/Q and therefore to predict the thermal force noise at a given temperature. Unfortunately, we have direct experimental access only to the apparent quality factor Q_a, which is affected by the SQUID-induced magnetic spring. In general, we have $1/Q_a = 1/Q + 1/Q_{SQ}$, where $1/Q_{SQ}$ represents the SQUID effect. It is theoretically expected that, in the limit of large feedback gain:

$$1/Q_{SQ} = c/|G| \tag{S2}$$

where $|G|$ is the open loop gain of the SQUID feedback electronics, and c is a coupling constant depending on the SQUID working point. This relation is easily derived by noting that the magnetic spring k_{SQ} induced by the SQUID arises from the effective flux $\Phi = \Phi_x x$ applied to the SQUID by the cantilever motion, which in turns generates a current J circulating around the SQUID loop through the responsivity $J_\Phi = \frac{dJ}{d\Phi}$ and a back-action force through the coupling $F_J = dF/dJ$. In absence of flux feedback, k_{SQ} can be written as :

$$k_{SQ} = \frac{dF}{dx} = F_J J_\Phi \Phi_x = J_\Phi \Phi_x^2 \tag{S3}$$

where $F_J = \Phi_x$ because of reciprocity, and J_Φ is the only quantity depending on the SQUID working point. When feedback is applied, the effective flux applied to the SQUID, and therefore the magnetic spring, is reduced by a factor $1/\left[1 + G\left(\omega\right)\right]$ where $G\left(\omega\right)$ is the open loop gain. In general $G\left(\omega\right)$ is complex, so that the spring features both a real and an imaginary part, leading respectively to a frequency shift Δf_{SQ} and a dissipation $1/Q_{SQ}$. Both components are proportional to $1/|G|$ for large $|G|$ and fixed argument. Thus, by varying the magnitude $|G|$ it is possible to distinguish $1/Q_{SQ}$, according to Eq. (S2). In particular, for $1/|G| \to 0$ the magnetic spring vanishes, allowing the intrinsic quality factor Q to be estimated.

The apparent quality factor Q_a is measured by using a standard ringdown method. Fig. S3 shows the measurements of Q_a as function of $1/|G|$ at different temperatures, corresponding to the data points of Fig. 3. We could not measure Q_a at larger gain (lower $1/|G|$) because of the onset of the principal feedback instability. All datasets are in very good agreement with the expected linear behaviour. Moreover, all slopes obtained from a linear fit are consistent within the error bar, as expected given that the SQUID working point was the same across all measurements.

UNCERTAINTY BUDGET ON T AND Q AND POSSIBLE SYSTEMATIC ERRORS

The quality factor $1/Q$ at a given temperature is estimated as the intercept of a linear fit to the datasets in Fig. S3. The error bar is obtained from the standard error on the fitting parameter. Because of the low number of points, the error bar is enlarged by a factor 1.32, cor-

responding to the 1σ (i.e. 68% probability) confidence interval of a Student's t-distribution with 2 degrees of freedom.

The measurement of T is based on a SQUID-based noise thermometer, which has been further calibrated against a superconducting reference point thermometer with accuracy better than 0.5% (HDL1000 Measurement System, http://hdleiden.home.xs4all.nl/srd1000). The noise thermometer is semiprimary (as it needs only one calibration point) and is simultaneously consistent with all reference points in the range 21 mK - 1.1 K, so its effective accuracy could be even better, but we take as conservative accuracy the value 0.5% set by the reference point device.

The x-error bars on T/Q in Fig. 3 (and in Fig. S5, S7) are obtained by combining in quadrature the relative error on $1/Q$ with the estimated accuracy $\delta T/T = 0.005$ on the measurement of T. The uncertainty on T is practically negligible with respect to the uncertainty on Q. As the uncertainties on the x-axis and the y-axis in Fig. 3 are both significant, the linear fit of the noise data is performed as a weighted orthogonal fit which takes simultaneously into account both uncertainties. The goodness of the fit is checked by means of a standard χ^2-test, which gives a regular value $\chi^2 = 9.27$ with 8 degrees of freedom. This is a good indication that the error bars are correctly estimated.

Concerning the estimation of $1/Q$ described above, any possible systematic error on the measurement procedure based on varying the open loop gain would be the same for any dataset, as all ringdown measurements of Q_a are performed in the same way at the same settings of the SQUID electronics. One may ask whether a common unknown constant bias on $1/Q$ would be potentially able to explain the nonzero intercept in the noise data of Fig. 3. To check this possibility, we have manually added a constant additional offset $1/Q_0$ to the data, and repeated the whole data analysis. It turns out that it is indeed possible to reduce the intercept to 0 for $1/Q_0 \simeq 1.1 \times 10^{-7}$, which is roughly 10 times larger than the average error bar on $1/Q$. However, for such a choice, the data deviate significantly from the linear behaviour, as we obtain $\chi^2 = 26$ with a relative probability of 0.001. Furthermore, we find that by varying $1/Q_0$ the χ^2 is actually minimized for a much lower offset $1/Q_0 = -7 \times 10^{-9}$, which is consistent with the error bar. In other words, under the assumptions that the data follow a linear relation, the likelihood of the observed data given an arbitrary $1/Q_0$ is essentially maximized by the choice $1/Q_0 \simeq 0$ (no systematic error). This is a further indication that the accuracy of the estimation of $1/Q$ is well within the measurement error bar.

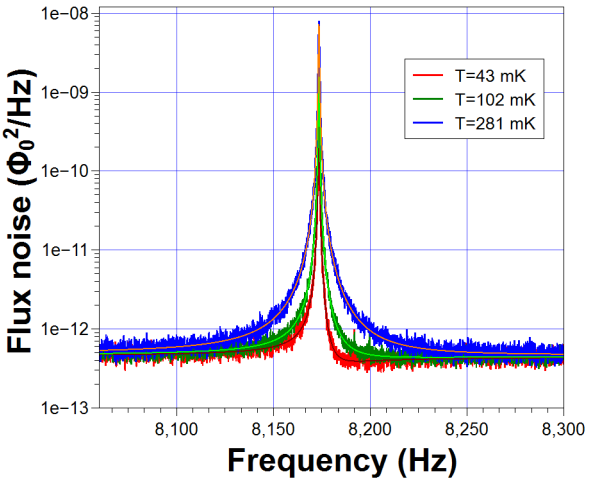

FIG. S4: Three representative spectra of the noise acquired in the high coupling run. The best fits with Eq. (2) are also shown.

MEASUREMENTS WITH HIGHER COUPLING

High coupling measurements were performed in a separate cooldown. The relative position of the cantilever with respect to the SQUID was carefully changed under the microscope and the system reassembled without other modifications.

The measurements were performed in similar way to the main run, but with a lower number of temperature points. Because of higher coupling the effective bandwidth of the cantilever noise was larger, leading in turn to a smaller error bar on the fitting parameters. Fig. S4 shows three representative spectra. The data are again fitted by Eq. (2). The χ^2 is well within the 2σ interval of the theoretical distribution for all spectra.

Fig. S5 shows the B parameter extracted from the fits as a function of T/Q. An orthogonal linear fit of the data leads to $B_0 = (4.3 \pm 0.4) \times 10^{-19}\ \Phi_0^2/\mathrm{Hz}$ and $B_1 = (0.872 \pm 0.007) \times 10^{-19}\ \Phi_0^2/(\mathrm{nK} \cdot \mathrm{Hz})$. The reduced χ^2 with 4 degrees of freedom is 0.21, which falls within the 2σ interval of the theoretical distribution. The coupling factor and the residual force noise inferred from B_0 and B_1 are reported in the second row of Table I.

MEASUREMENTS WITH PULSE TUBE ON

During the same cooldown of the main measurements, we have performed additional measurements without switching off the pulse tube cryocooler. Under normal operation, the high pressure pulses at frequency ~ 1.5 Hz generated by the pulse tube compressor are by far the strongest source of vibrational noise in our cryostat.

Typically, we observe two different effects. On the one hand there is a direct generation of vibrational noise at the mixing chamber plate level, extending up to the 10

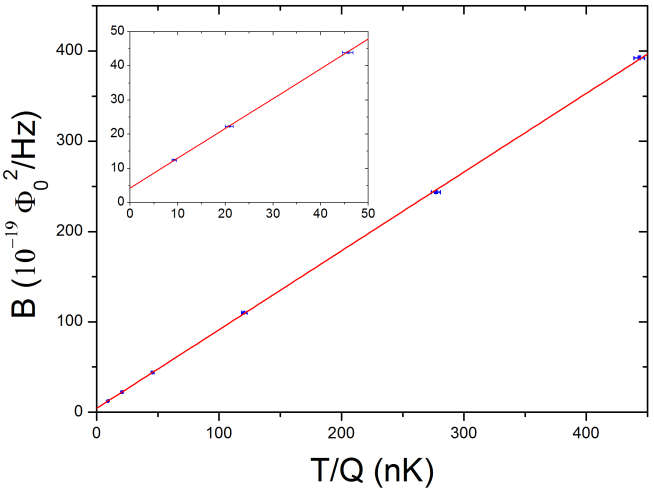

FIG. S5: B parameter as a function of T/Q for the high coupling dataset. The lowest points are zoomed in the inset. A linear fit is fully consistent with the data, yielding a finite intercept.

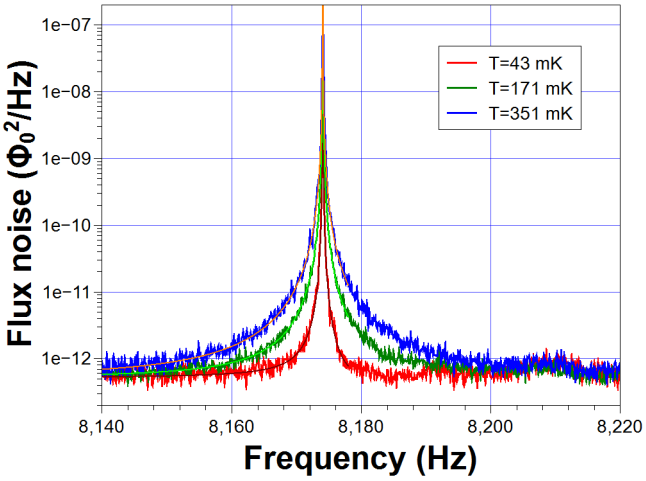

FIG. S6: Three representative spectra of the noise acquired with pulse tube on. Several bumps are apparent on the right tail. The best fit with Eq. (2) are also shown. The fit is restricted to $f < 8178$ Hz and the parameters A and C are fixed to the values obtained with pulse tube off.

kHz region, which can be directly measured by standard accelerometers. At the cantilever frequency the acceleration noise is less than 10^{-5} $g/\sqrt{\text{Hz}}$ and our suspension system provides a factor $\sim 10^4$ attenuation. As the effective mass of our cantilever is $\sim 10^{-10}$ Kg, this translates into a force noise ~ 1 aN$/\sqrt{\text{Hz}}$, thus comparable or lower than our residual measured force noise. The noise with pulse tube off is at least a factor of 10 better (a factor 100 in power).

On the other hand, very high vibrational noise levels are sometimes observed at the cantilever frequency due to nonlinear upconversion of low frequency noise. Upconversion is a poorly understood and rather unpredictable effect. It is highly nonstationary and threshold-like, with the noise at the resonator frequency which can vary by orders of magnitude, depending on the magnitude of the low frequency motion. We have evidence that upconversion is related either with soft thermal links or with the SQUID braided cable. We have been able to strongly reduce upconversion noise by implementing a passive magnetic damper in the suspension system, to reduce the low frequency motion, and by a proper clamping of the SQUID wiring. In particular, in the cooldown here considered, nonlinear upconversion was essentially absent even with the pulse tube on.

Fig. S6 shows three representative spectra acquired with the pulse tube on, with the same acquisition settings of the main measurements run. Several broad bumps are apparent on the right tail of the resonator peak, while the left tail is rather clean. A global fit yields a χ^2 unacceptably high, which confirms the presence of coloured vibrational noise. However, we obtain acceptable χ^2 by excluding a wide portion of the right tail from the fit, as shown in Fig. S6. By applying the standard data analysis we obtain again a good linear behaviour of B as a function of T/Q, as shown in Fig. S7. The slope of the linear fit $B_1 = (0.286 \pm 0.003) \times 10^{-19}$ $\Phi_0^2/\text{Hz} \cdot \text{nK}$ is consistent with the one at pulse tube off, while the intercept $B_0 = (1.71 \pm 0.13) \times 10^{-19}$ Φ_0^2/Hz leads to a larger residual force noise (see Table I).

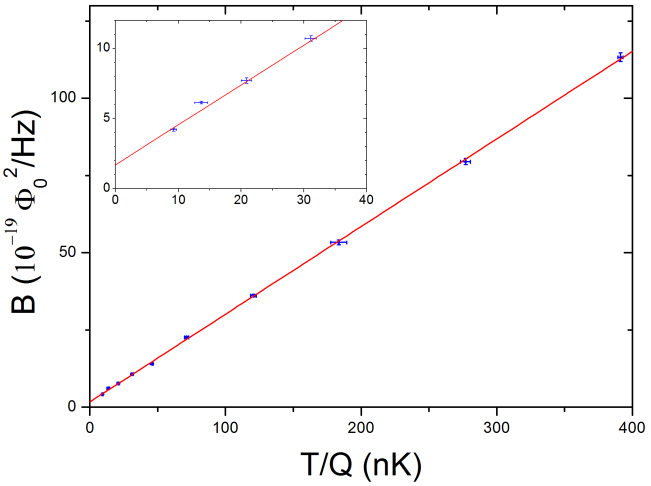

FIG. S7: B parameter as a function of T/Q for the measurements with pulse tube on. The lowest points are zoomed in the inset. A linear fit is again consistent with the data, yielding a finite intercept.

MEASUREMENTS WITH PUMP OFF

Under pulse tube off operation, the stronger source of vibrational and acoustic noise is the roots mechanical pump which is employed to circulate the ^{3}He-^{4}He

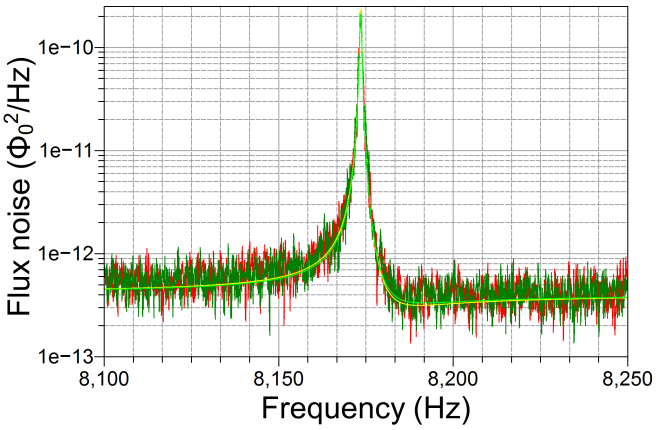

FIG. S8: Spectra acquired with circulation pump on (red line) and off (dark green line). The pulse tube is off. Both measurements are performed under the same conditions, with the same number of averages. The best fit with Eq. (2) is also shown. No significant difference in the fitting parameters is observed.

mixture in the dilution refrigerator. We have tried to investigate whether the pump noise can be related to the observed cantilever excess noise. The measurement was performed during a separate cooldown with the high coupling setting at the lowest temperature $T = 43$ mK.

Unfortunately, it is not possible to maintain a stable temperature for long time after switching off the circulation pump. The cooling power drops to zero very quickly and the temperature starts drifting after a time of the order of 1 minute. In contrast, we can easily operate the dilution refrigerator with pulse tube off up to half an hour while keeping the temperature of the mixing chamber actively stabilized. In order to collect significant statistics while keeping a stable temperature, we switch off the circulation pump for short periods (about 40 seconds), barely sufficient to wait for the low frequency suspension modes to relax and acquire one single data frame. Subsequently we switch the pump on, wait several minutes for the circulation to stabilize and then repeat the procedure. We collected a total of 12 acquisitions. The averaged spectrum is then compared with a spectrum with circulation pump on. For a fair comparison, the spectrum with pump on is acquired with the same setting and the same number of averages.

The two spectra are shown in Fig. S8, and can be hardly distinguished. The best fitting curves are also shown and are essentially coincident. The B parameters resulting from the fits are $B = (1.26 \pm 0.04) \times 10^{-18}$ Φ_0^2/Hz and $B = (1.29 \pm 0.04) \times 10^{-18}$ Φ_0^2/Hz for the pump on and pump off case respectively. Therefore, there is apparently no significant effect of the circulation pump on the excess noise, which at this temperature contributes to about 30% of B.

MAGNETIC EFFECTS

As the ferromagnetic microsphere is magnetized, an external magnetic field noise could be also held responsible for anomalous force driving the cantilever. Let us assume an environmental magnetic noise B_n with direction along the cantilever length and negligible spatial dependence over the magnetic sphere volume. B_n would generate a torque μB_n, where $\mu \simeq 5 \times 10^{-9}$ J/T is the microsphere magnetic moment, which translates into an effective force noise $\mu B_n/l$, where l is the effective length of the cantilever. Under these assumptions, the observed excess force noise would result from a magnetic field noise B_n with spectral density 1×10^{-13} T/$\sqrt{\text{Hz}}$. Such noise is typical of an unshielded environment at kHz frequency, but is unrealistically large for a shielded environment. The walls of the copper box hosting the cantilevers are about 20 times thicker than the penetration depth at the cantilever frequency, thus providing an attenuation of external magnetic fields by many orders of magnitude. Thermal magnetic noise from eddy currents in the walls or other elements inside the box is estimated to be largely negligible.

A related but distinct mechanism is given by fluctuations of the microsphere magnetization. The magnetic microsphere is at finite temperature, so there will be magnetization fluctuations, which will couple to the static magnetic field yielding a finite torque and force noise. Magnetization fluctuations for a fully magnetized hard ferromagnet are expected to be very small, due to the very high anisotropy field. Experiments with rare-earth micromagnets have actually shown that at kHz frequency a larger effect is due to conductive eddy currents [36]. Along with the approach of [36] we estimate both effects to be many orders smaller than what is needed to explain the observed force noise. For instance, the eddy current dissipation in the microsphere can be calculated analytically and is 6 orders of magnitude smaller than the cantilever mechanical dissipation.

However, we can also provide an experimental argument to rule out this mechanism. Magnetization fluctuations would behave as thermal force noise and the same mechanism would also appear as mechanical dissipation. In particular, both noise and dissipation would scale with the square of the external magnetic field. In a separate test we have have increased the external magnetic field by a factor 4 with respect to the earth field. We did not see any significant change of the quality factor, confirming that thermal magnetization fluctuations are likely not significant in our experiment.